Research Article   **Open Access**

Study the Interaction between Gold Nanoparticles and Bovine Serum Albumin: Spectroscopic Approach

Husain Alsamamra*, Ibrahim Hawwarin, Sawsan Abu-Sharkh and Musa Abuteir

Physics Department, Al-Quds University, Palestine

Abstract

Interaction between gold nanoparticles of 40 & 60 nm with BSA has been investigated using UV-absorption spectrophotometry, fluorescence spectroscopy and FT-IR spectroscopy. UV-absorption spectrophotometry showed an increase in the absorption intensity with increasing the molecular ratios of gold nanoparticles of both sizes to BSA, it is found that the value of the binding constant is estimated to be 0.888×10^4 M^{-1} for gold nanoparticles (40 nm)-BSA complexes, and 1.16×10^4 M^{-1} for gold nanoparticles (60 nm)-BSA complexes. FT-IR spectroscopy analysis showed that intensities of gold nanoparticles of both sizes-BSA complexes decrease as the concentration increased.

Introduction

Gold nanoparticles (AuNPs) have drawn remarkable interest in the past few years because of their potential applications in biomedicines [1,2], biotechnology [3,4], electronics [5], and catalysis [6], this is due to many attractive properties, such as excellent conductivity, size-dependent properties, optical properties, non-toxicity, and their capacity for facile and highly variable functionalization. Recently, stabilization of AuNPs by a variety of biomolecules such as proteins, peptides, DNA, and carbohydrates has been of great interest due to their applications in biomedicine including diagnostics, bio-imaging and targeted drug delivery [7].

The conjugation of proteins with AuNPs not only affords stabilization of the system but, more importantly, also introduces biocompatible functionalities into these AuNPs for further biological interactions. The surface modifications of AuNPs to provide stable bimolecular functionalized AuNPs in biomedical applications have been reported by various groups [2,6-8]. On the other hand, antibody–antigen binding is a fundamental phenomenon in the fields of biochemistry and biology. Most bioassays are based on an antibody–antigen binding pair [9].

Serum albumin is the major protein component of blood plasma but is distributed to the interstitial fluid of the body tissues [10]. Serum albumin is capable of binding to a wide variety of drugs, and there is strong interest in this abundant protein because of its effects on drug delivery [11]. Therefore, immobilization and immunoreaction of a fundamental protein, such as serum albumin on gold NPs, is very important for bio applications.

To design an effective AuNPs-protein system for biological applications, it is necessary to study the AuNPs-protein interactions systematically. Some studies have investigated the influence of AuNP size on the conformation of cytochrome [12]; and the effect of pH on the conformation of BSA adsorbed on the surface of AuNPs [13-16]. Fluorescence spectroscopy [11,14], dynamic light scattering [8,17], circular dichroism [9,18], Fourier transform infrared spectroscopy (FTIR) [19], nuclear magnetic resonance spectroscopy [20], surface enhanced Raman scattering [21], time-correlated single photon counting spectroscopy [13,22] are among a variety of techniques commonly used to characterize AuNPs-protein interactions. The combination of different techniques will give us insight into the interactions of AuNPs and proteins [16].

Bovine serum albumin (BSA) is a model globular protein which is widely used in biochemical studies [20,21]. It is composed of 583 amino acid residues containing several sulfur, oxygen and nitrogen atoms, which are generally used to stabilize the nanoparticles [22]. BSA plays a significant role in many important physiological functions, and its structure and conformation can be easily changed [23]. AuNPs-BSA bio conjugates have been used in several applications such as intracellular delivery vectors and imaging agents [24]. Fundamental studies on the interactions between AuNPs and BSA may contribute to development of optimal conditions for forming bio conjugated nanomaterials that preserve the functionality of proteins.

In this study, BSA was conjugated with AuNPs (40 and 60 nm) and the interactions between them were studied by UV-visible absorption spectroscopy, fluorescence spectroscopy and Fourier transform infrared spectroscopy (FT-IR). Based on the data obtained using these techniques, the effects of BSA concentration on the stability of the AuNPs and the conformational changes of BSA upon interacting with the AuNPs are discussed, and a possible mechanism of the conjugation is proposed.

Samples and Methods

BSA and gold nanoparticles in powder form were purchased from Sigma Aldrich chemical company and used without further purifications. The data were collected using samples in the form of thin films for FT-IR measurements and liquid form for UV-VIS and fluorescence measurements.

Preparation of stock solutions

BSA was dissolved in phosphate buffer saline, at physiological pH 7.4, to a concentration of (80 mg/ml), to get a final concentration of (40 mg/ml). Gold nanoparticles with molecular weight (288.42 g/mol) was dissolved in phosphate buffer saline (0.7622 mg/ml), the phosphate

*Corresponding author: Husain Alsamamra, Physics Department, Al-Quds University, Palestine, Tel: 00972-5297166009; E-mail: hsamamra@staff.alquds.edu

buffer saline was at room temperature, the solution were placed on a shaker for 1 h in order to dissolve the gold nanoparticles powder with buffer, then it was placed in ultrasonic water path (SIBATA AU-3T) for 8 h to ensure that the entire amount of gold nanoparticles was completely dissolved. The solution was placed in a water path with a temperature range 37-40°C for 1 h to let the solution completely dissolved and became homogenous. The final concentrations of BSA-Gold nanoparticles solutions were prepared by using the following molecular ratios of BSA: Gold nanoparticles; 10:18, 10:14, 10:10, 10:6 and 10:2.

UV-absorption spectrometer

A 1 μl sample of gold nanoparticles is pipetted into the end of a fiber optical cable (the receiving fiber). A second fiber optical cable (the source fiber) is then brought into contact with the liquid sample causing the liquid to bridge the gap between the fiber optical ends. The gap is controlled to both 1 mm and 0.2 mm paths. A pulsed xenon flash lamp provides the light source and a spectrophotometer utilizing a linear CCD array is used to analyze the light after passing through the sample. The absorption spectra were recorded for free BSA and for its complexes with gold nanoparticles. Repeated measurements were done for all samples.

Fluorescence spectrometer

A 2.5 μl sample of gold nanoparticle is pipetted onto the end of the lower measurement pedestal (the receiving fiber). A non-reflective "bushing" attached to the arm is then brought into contact with the liquid sample causing the liquid to bridge the gap between it and the receiving fiber. The gap, or path-length, is controlled to 1 mm. following excitation with one of the three LEDs; emitted light from the sample passing through the receiving fiber is captured by the spectrophotometer.

FT-IR spectrometer

The absorption spectra were obtained in the wave number range of 400-400 cm^{-1}. A spectrum was taken as an average of 60 scans to increase the signal to noise ratio, and the spectral resolution was at 4 cm^{-1}. The aperture used in this study was 8 mm, since we found that this aperture gives best signal to noise ratio. Baseline correction, normalization and peak areas calculations were performed for all the spectra by OPUS software. The peak positions were determined using the second derivative of the spectra. The infrared spectra of BSA, Gold nanoparticles-BSA complexes were obtained in the region of 1000-1800 cm^{-1}. The FT-IR spectrum of free BSA was acquired by subtracting the absorption spectrum of the buffer solution from the spectrum of the protein solution. For the net interaction effect, the difference spectra {(protein and gold nanoparticles solution)-(protein solution)} were generated using the featureless region of the protein solution 1800-2200 cm^{-1} as an internal standard.

Results and Discussion

UV-absorption spectrometer

The absorption spectra of different ratios of gold nanoparticles (40 and 60 nm) with fixed amount of BSA are displayed in Figures 1 and 2. The excitation has been done on 210 nm and the absorption is recorded at 278 nm. The figures shows that the intensity of BSA increases with the increasing of gold nanoparticles percentage, and that the absorption peaks of these solutions showed moderate shifts indicating that with the addition of gold nanoparticles, the peptide
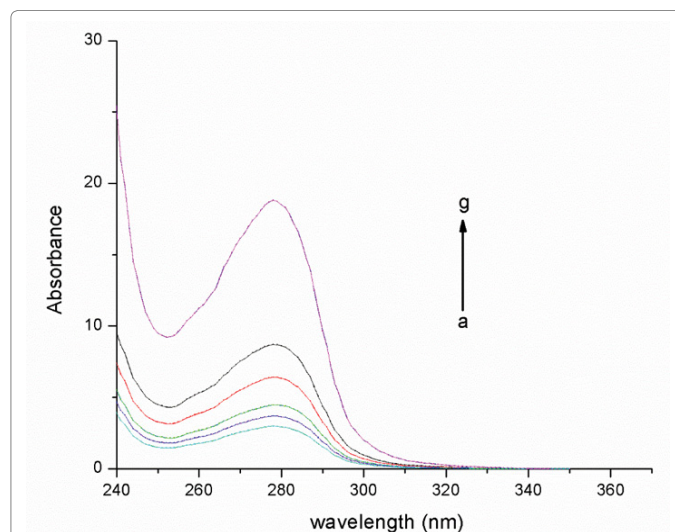
Figure 1: UV-absorbance spectra of BSA with different molar ratios of gold nanoparticles (40 nm) (a=0:10, b=2:10, c=6:10, d=10:10, e=14:10, f=18:10, g= free gold nanoparticles).
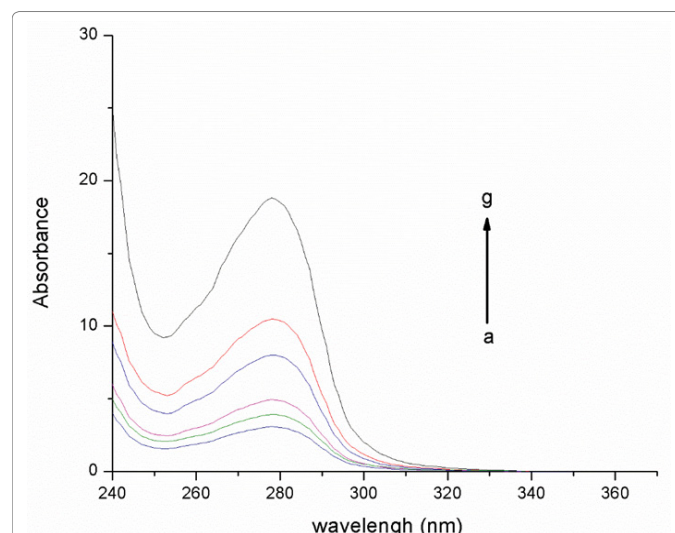
Figure 2: UV-absorbance spectra of BSA with different molar ratios of gold nanoparticles (60 nm) (a=0:10, b=2:10, c=6:10, d=10:10, e=14:10, f=18:10, g= free gold nanoparticles).

strands of BSA molecules extended more and the hydrophobicity of gold nanoparticles was decreased. The result support that the peak shifts between free BSA solution and gold nanoparticles-BSA complexes are due to the interaction between gold nanoparticles and BSA. Repeated measurements were done for all the samples showing consistent results and no significant differences were observed.

Gold nanoparticles -BSA complexes binding constants were determined using UV- spectrophotometer [20], by assuming that there is only one type of interaction between gold nanoparticles-BSA complexes, which leads to establish Equations 1 and 2 as follows:

BSA+Gold nanoparticles $\leftrightarrow$ Gold nanoparticles: BSA   (1)

K = [Gold nanoparticles: BSA]/[Gold nanoparticles] [BSA]   (2)

The absorption data were treated using linear double reciprocal plots based on the following equation:

$$1/A-A_0=1/A_\infty-A_0+1/K[A_\infty-A_0].1/L \qquad (3)$$

Where A_0 corresponds to the initial absorption of protein at 280 nm in the absence of ligand, A_∞ is the final absorption of the ligated protein, and A is the recorded absorption at different gold nanoparticles concentrations (L). The double reciprocal plot of $1/(A-A_0)$ *vs.* 1/L is linear as it shown in Figures 3 and 4.

The binding constant (K) can be estimated from the ratio of the intercept to the slope to be (0.888×10^4 M^{-1}) for gold nanoparticles (40 nm)-BSA complexes, and (1.16×10^4 M^{-1}) for gold nanoparticles (60 nm)-BSA complexes. The value obtained is indicative a weak gold nanoparticles protein interaction with respect to the other drug-BSA complexes with binding constant in the range of 10^5 and 10^6 M^{-1} [22].

Fluorescence spectrophotometer

In this work, BSA-Gold nanoparticles complexes excitation wavelength at 360 nm was used, and the observed wavelength emission was at 439 nm. The fluorescence sensor is based on intramolecular charge transfer (ICT), which is highly sensitive to the polarity of microenvironment. Therefore, it is expected to act as fluorescent probe for some biochemical systems like proteins.

The fluorescence quenching spectra of BSA at various percentages of gold nanoparticles (40 nm and 60 nm) are shown in Figures 5 and 6. Obviously from the results, the fluorescence intensity of BSA gradually decreased while the peak position shows little change upon increasing the percentage of gold nanoparticles, indicating that gold nanoparticles binds to BSA. Under the same condition, no fluorescence of gold nanoparticles was observed that indicates gold nanoparticles could quench the auto fluorescence of BSA and the interaction between gold nanoparticles and BSA exists.

Fluorescence quenching can be defined as a bimolecular process that reduces the fluorescence intensity without changing the fluorescence emission spectrum; it can result from transient excited-
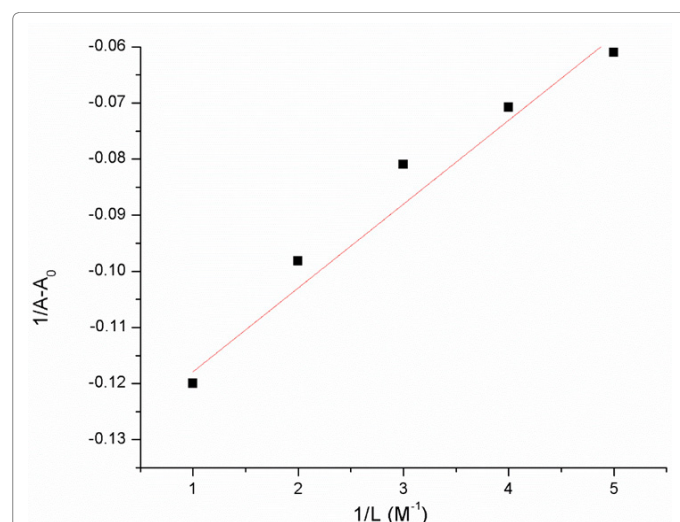

Figure 3: The plot of $1/A-A_0$ *vs.* 1/L for BSA with different concentrations of gold nanoparticles 40.
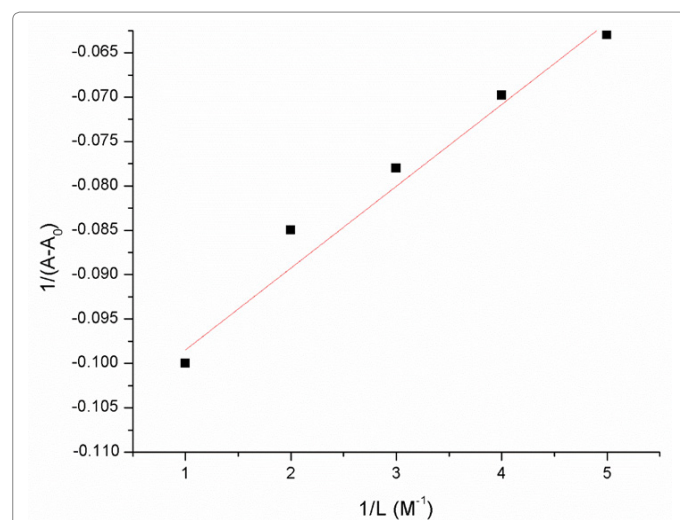
Figure 4: The plot of $1/A-A_0$ *vs.* 1/L for BSA with different concentrations of gold nanoparticles 60 nm.
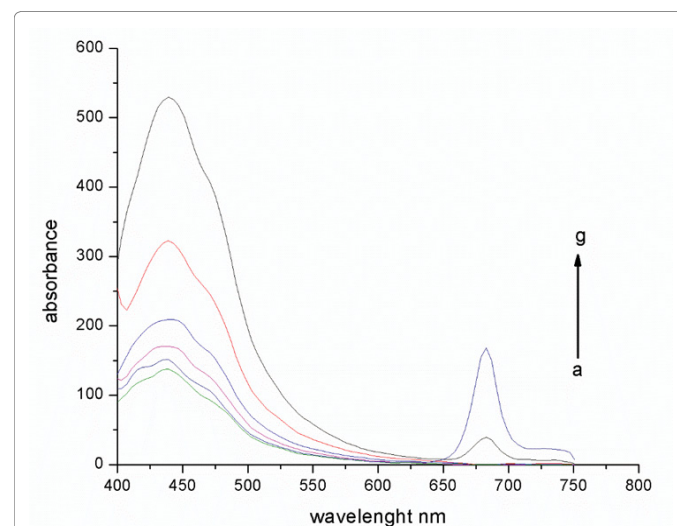
Figure 5: Fluorescence absorption spectra of BSA in the absence and presence of gold nanoparticles 40 nm in these ratios (a=0:10, b=2:10, c=6:10, d=10:10, e=14:10, f=18:10, g=free gold nanoparticles).
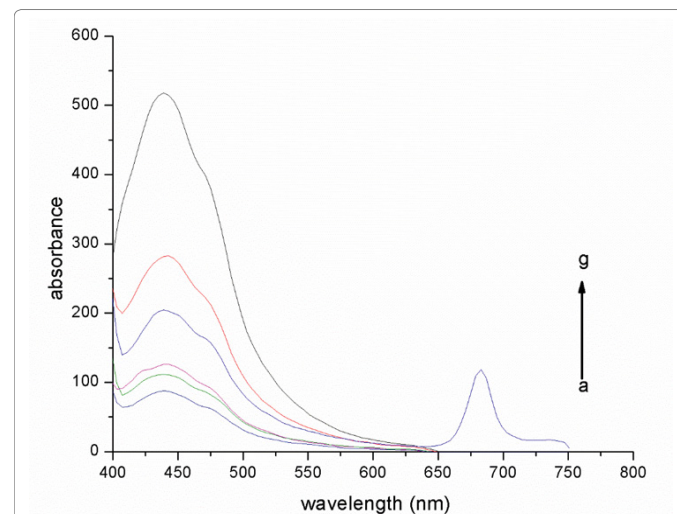
Figure 6: Fluorescence absorption spectra of BSA in the absence and presence of gold nanoparticles 60 nm in these ratios (a=0:10, b=2:10, c=6:10, d=10:10, e=14:10, f=18:10, g=free gold nanoparticles).

state interactions (collisional quenching) or from formation of non-fluorescent ground-state species.

For dynamic quenching, the decrease in fluorescence intensity is described by Stern-Volmer equation [20].

$$F_0/F = 1 + K_{sv}[L] = 1 + k_q\tau_0[L] \qquad (4)$$

In this expression F and F_0 are the fluorescence intensities with and without quencher, K_{sv} is the Stern-Volmer quenching constant, K_q is the bimolecular quenching constant, τ_0 is average lifetime of the biomolecule without quencher, and (L) is the quencher concentration. The Stern-Volmer quenching constant K_{sv} indicates the sensitivity of the fluorophore to a quencher.

The Stern-Volmer quenching constant K_{sv} was obtained by the slope of the curves obtained in Figures 7 and 8, and its value equals (2.17×10^2 L mol^{-1}) for gold nanoparticles 40 nm-BSA complexes. From the equation the value of $K_{sv} = Kq^{\cdot}\tau_0$, from which we can calculate the value of K_q using the fluorescence life time of 10^{-8} s for BSA [16], to obtain K_q value of (2.17×10^{10} Lmol^{-1}s^{-1}) for gold nanoparticles-BSA complexes.
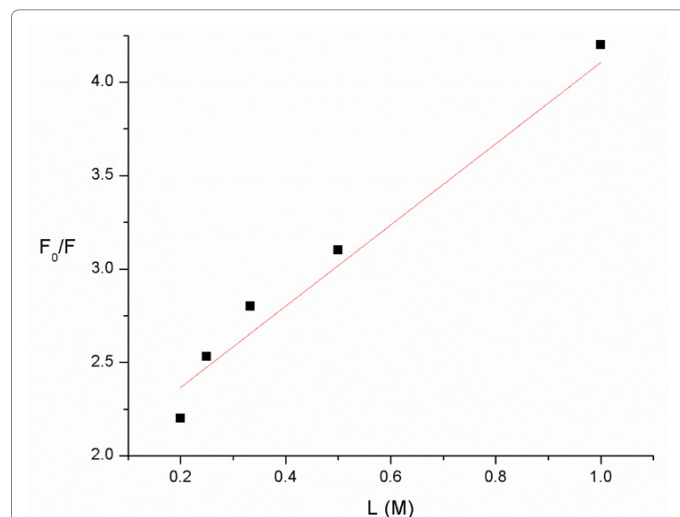
The value of K_{sv} for gold nanoparticles 60 nm-BSA complexes (4.5×10^2 Lmol^{-1}). However, the value of K_q (4.5×10^{10} Lmol^{-1}s^{-1}) which is larger than the maximum dynamic quenching constant for various quenchers with biopolymer (2×10^{10} Lmol^{-1}s^{-1}). This implies that the quenching is not initiated by dynamic collision but from formation of a complex, so static quenching is dominant.

For static quenching, the following equation is used to determine the binding constant between BSA and gold nanoparticles.

$$1/(F_0-F) = 1/F_0K(L) + 1/F_0 \qquad (5)$$

Where K is the binding constant of gold nanoparticles with BSA, and can be calculated by plotting $1/(F_0-F)$ vs. 1/L. As shown in Figures 8 and 9, the value of K equals the ratio of the intercept to the slope. The obtained value of K equals (0.92×10^4 M^{-1}, 1.3×10^4 M^{-1}) respectively from Figures 9 and 10 which agree well with the value obtained earlier UV spectroscopy and supports the effective role of static quenching.
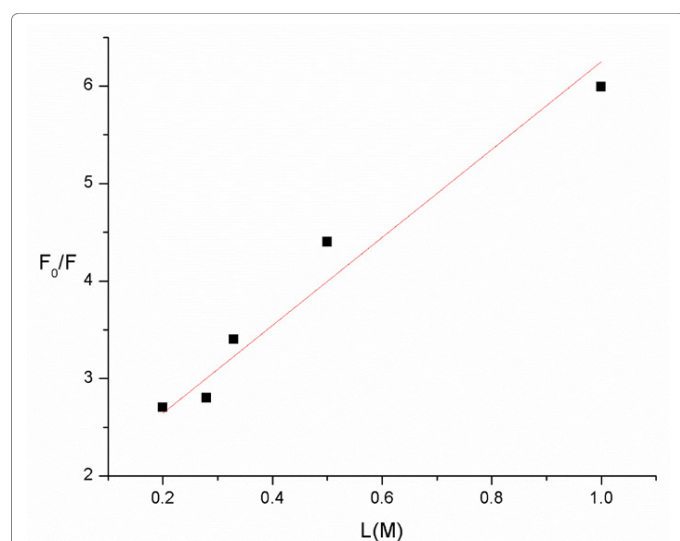
The acting forces between a small molecule substance and macromolecule mainly include hydrogen bond, Van der Waals forces',
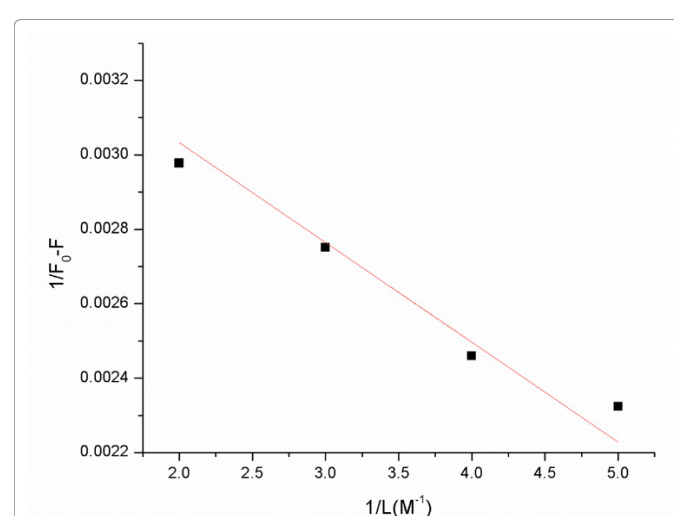

Figure 7: The Stern Volmer plot for gold nanoparticles 40nm –BSA complexes.
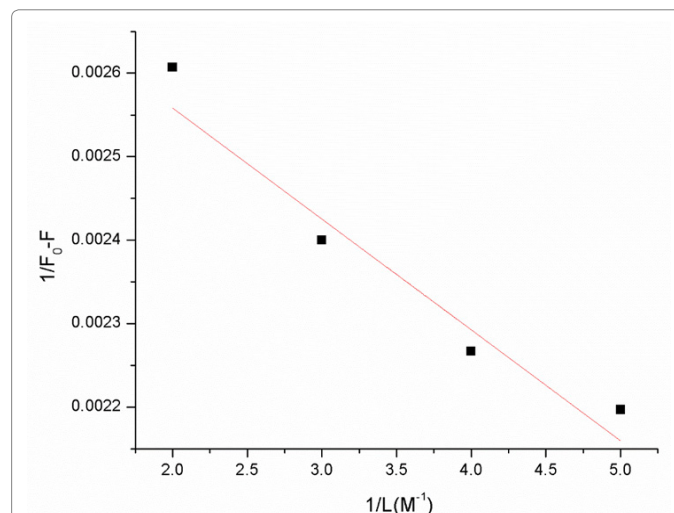
Figure 9: The plot of $1/F_0-F$ vs. (1/L) ×10^4 for gold nanoparticles 40 nm–BSA complexes.

Figure 8: The Stern Volmer plot for gold nanoparticles 60 nm –BSA complexes.

Figure 10: The plot of $1/F_0-F$ vs. (1/L) ×10^4 for gold nanoparticles 60 nm–BSA complexes.

electrostatic force and hydrophobic interaction force. It was more likely that hydrophobic and electrostatic interactions were involved in the binding process.

However, gold nanoparticles might be largely unionized under the experimental conditions, as expected from its structure. Hence, electrostatic interaction could be precluded from the binding process. Thus, the binding of gold nanoparticles to BSA includes the hydrophobic interaction. Hydrophobic interaction is mostly an entropic effect originating from the disruption of highly dynamic hydrogen bonds between molecules of liquid water by the nonpolar solutes. Minimizing the number of hydrophobic side chains exposed to water is the principal driving force behind the folding process. Formation of hydrogen bonds within the protein stabilizes protein structure [23].

FT-IR Spectroscopy

FT-IR spectroscopy provides information about secondary content of proteins; this information arises from the amide band which is a result from the vibrations of the groups around the peptide bonds of proteins. Changes in hydrogen bonding involves in the peptide linkages would occur, this results in changes of vibrational frequency of the different amide modes when the binding between drugs and globular protein like BSA occurs.

As shown in Figure 11, the infrared spectrum of protein is characterized by a set of absorption the amide region and the C-H region. The modes most widely used in protein structural studies are amide I, amide II and amide III.

Amide I band ranging from 1700 to 1600 cm^{-1} and arises principally from the C=O stretching. Amide II band is primarily N-H bending with a contribution from C-N stretching vibrations, amide II ranging from 1600-1480 cm^{-1}. Amide III band ranging from 1330-1220 cm^{-1} which is due to the C-N stretching mode coupled to the in-plane N-H bending mode. This absorption is normally weak.

As Figures 12 and 13 provides, it is obviously seen as gold nanoparticles ratio were increased the intensities of the amide I, amide II and amide III bands decreased further in the spectra of all gold nanoparticles BSA complexes. The reduction in the intensity of the three amide bands is related to the gold nanoparticles BSA interaction.

In Table 1 the peak positions of BSA with different ratios of gold nanoparticles (40 nm) are listed. For gold nanoparticles (40 nm)-BSA
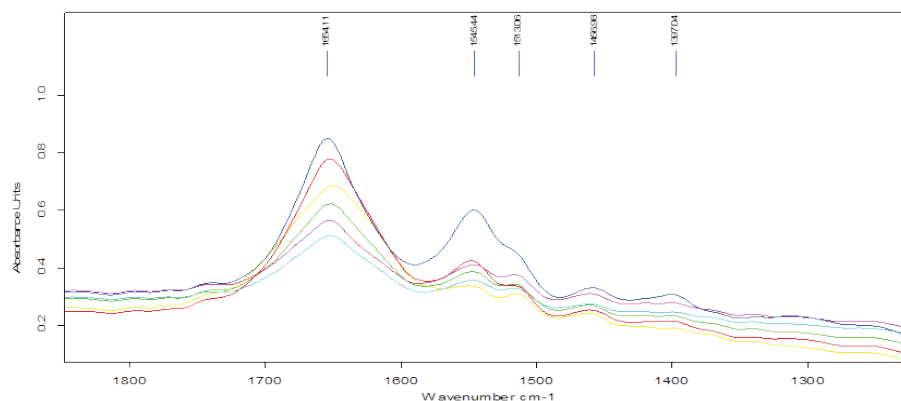
interaction the amide bands of BSA infrared spectrum shifted, for amide I band the peak positions have shifted as follows: 1621 cm^{-1} to 1629 cm^{1},1654 cm^{-1} to 1658 cm^{-1}. In amide II the peak positions have shifted as follows: 1513 cm^{-1} to 1523 cm^{-1} and 1579 cm^{-1} to 1583 cm^{-1}, in addition new peaks have been appeared at high molecular ratios of gold nanoparticles at 1547 cm^{-1} and 1569. In amide III region the peak positions are also have been shifted as the following order: 1242 cm^{-1} to 1241 cm^{-1}, 1314 cm^{-1} to 1315 cm^{-1},1339 cm^{-1} to 1335 cm^{-1} and 1366 cm^{-1} to 1361 cm^{-1}.

In Table 2 the peak positions of BSA with different ratios of gold nanoparticles (60 nm) are listed. For gold nanoparticles(60 nm)-BSA interaction the amide bands of BSA infrared spectrum shifted as listed in the table, for amide I band the peak positions have shifted as follows: 1621 cm^{-1} to 1626 cm^{1},1654 cm^{-1} to 1655 cm^{-1}. In amide II the peak positions have shifted as follows: 1513 cm^{-1} to 1516 cm^{-1} and 1579 cm^{-1} to 1581 cm^{-1}, in addition new peaks have been appeared at high molecular ratios of gold nanoparticles at 1545 cm^{-1} and 1557. In amide III region the peak positions are also have been shifted as the following order: 1242 cm^{-1} to 1241 cm^{-1}, 1314 dos not change, 1339 cm^{-1} to 1332 cm^{-1} and 1366 cm^{-1} to 1357 cm^{-1}.

To summarize, the binding of gold nanoparticles of both sizes to BSA has been investigated by UV-absorption spectroscopy, fluorescence spectrometry and by FT-IR spectroscopy. From the UV and fluorescence investigations, we determined the values for the binding constants and the quenching constant. The FT-IR analysis reveals intensity reduction.
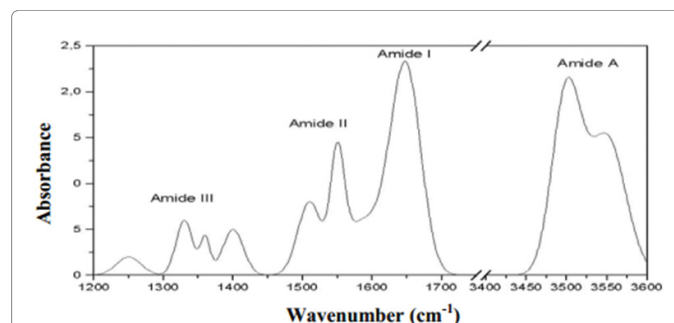
Figure 11: Sample spectrum showing the three relevant regions for determination of protein secondary structure. Amide I (1700-160 cm^{-1}), amide II (160-1480 cm^{-1}), amide III (1330-1220 cm^{-1}).

Figure 12: The spectrum of Gold nanoparticles 40 nm-BSA complexes with different percentage of gold nanoparticles.

Figure 13: The spectrum of Gold nanoparticles 60 nm-BSA complexes with different percentage of gold nanoparticles.
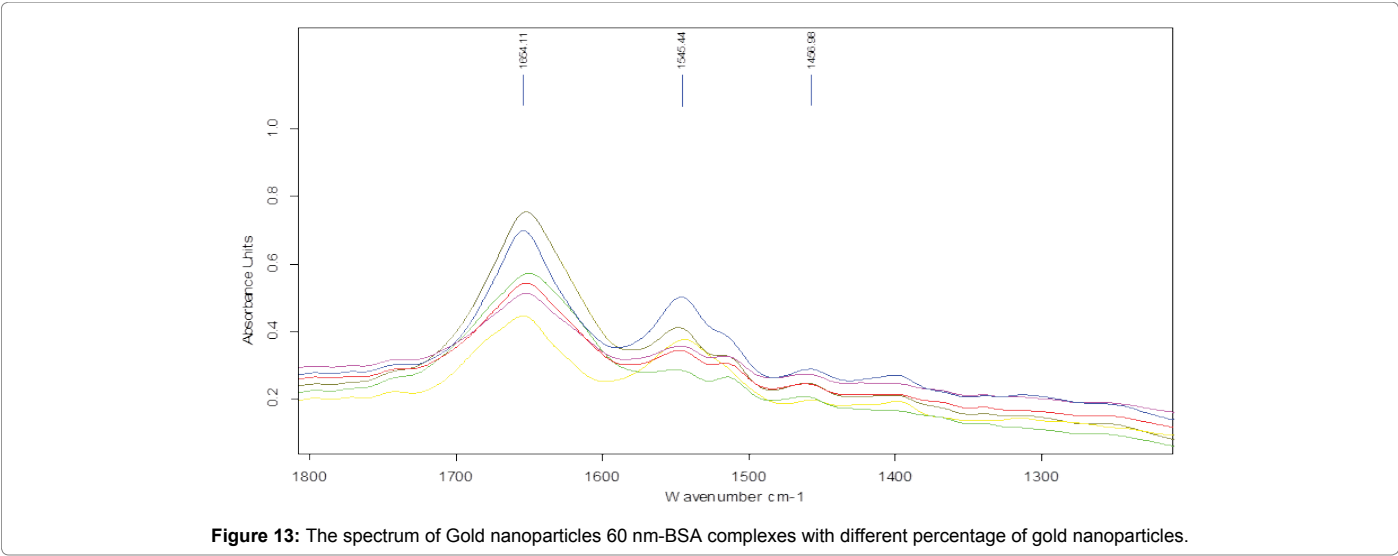
Bands	Free BSA	BSA - gold nanoparticles 01:01	BSA - gold nanoparticles 01:02	BSA - gold nanoparticles 01:03	BSA - gold nanoparticles 01:04	BSA- gold nanoparticles 01:05
amide I	1621	1622	1622	1628	1629	1629
(1700-1600)	1654	1654	1655	1657	1658	1658
amide II	1513	1513	1517	1521	1521	1523
(1600-1480)	1545	1548	1552	1559	1563	1569
	1579	1578	1578	1782	1782	1783
amide III	1242	1242	1241	1243	1241	1241
(1330-1220)	1314	1314	1341	1314	1316	1315
	1339	1339	1338	1337	1335	1335
	1366	1365	1364	1364	1362	1361

Table 1: Band assignment in the absorbance spectra of BSA with different gold nanoparticles (40 nm) molecular ratios for amide I, amide II, and amide III regions.

Bands	Free BSA	BSA - gold nanoparticles 1:1	BSA - gold nanoparticles 1:2	BSA - gold nanoparticles 1:3	BSA - gold nanoparticles 1:4	BSA - gold nanoparticles 1:5
amide I (1700-1600)	1621	1621	1622	1623	1623	1626
	1654	1654	1655	1655	1655	1655
amide II (1600-1480)	1513	1513	1514	1514	1515	1516
	1545	1547	1551	1552	1554	1557
	1579	1578	1578	1779	1781	1781
amide III (1330-1220)	1242	1242	1241	1242	1241	1241
	1314	1314	1314	1314	1314	1314
	1339	1339	1338	1337	1335	1332
	1366	13654	1361	1360	1359	1357

Table 2: Band assignment in the absorbance spectra of BSA with different gold nanoparticles (60 nm) molecular ratios for amide I, amide II, and amide III regions.

Conclusion

BSA plays a significant role in many important physiological functions, and its structure and conformation can be easily changed. Gold nanoparticles can easily form conjugates with proteins through either covalent bonds or physical interactions, and these conjugates have been widely applied in biomedical fields, including diagnostics, bio-imaging and targeted drug delivery. In order to design an effective gold nanoparticles-protein system for biological applications, it is necessary to study the gold nanoparticles-BSA interactions systematically. This is important for the application of the gold nanoparticles-BSA bio conjugates in nanobiosensors, disease diagnostics, drug delivery, biological labeling and imaging, and where biological activity is required.

References

1. Zhou X, Zhang X, Yu X, Zha X, Fu Q, et al. (2008) The effect of conjugation to gold nanoparticles on the ability of low molecular weight chitosan to transfer DNA vaccine. Biomaterials 29: 111-117.

2. Liu T, Tang J, Jiang L (2004) The enhancement effect of gold nanoparticles as a surface modifier on DNA sensor sensitivity. Biochem Biophys Res Commun 313: 3-7.

3. Medley CD, Smith JE, Tang Z, Wu Y, Bamrungsap S (2008) Gold nanoparticle-based colorimetric assay for the direct detection of cancerous cells. Anal Chem 80: 1067-1072.

4. Scampicchio M, Arecchi A, Mannino S (2009) Optical nanoprobes based on gold nanoparticles for sugar determination. Nanotechnology 20: 135501-135505.

5. Labande A, Ruiz J, Astruc D (2002) Supramolecular gold nanoparticles for the

redox recognition of oxoanions: syntheses, titrations, stereoelectronic effects, and selectivity. J Am Chem Soc 124: 1782-1789.

6. Liu Z, Hu P, Alavi A (2002) Catalytic role of gold in gold-based catalysts: a density functional theory study on the CO oxidation on gold. J Am Chem Soc 124: 14770-14779.

7. Hussain ST, Iqbal M, Mazhar M (2009) Size control synthesis of starch capped-gold nanoparticles. J Nanoparticle Res 11: 1383-1391.

8. Niemeyer CM (2001) Nanoparticles, proteins, and nucleic acids: Biotechnology meets materials science. Angew Chem Int Ed 40: 4128-4158.

9. Johnsona SR, Evans SD, Mahonb SW, A Ulmanc A (1997) Synthesis and characterisation of surfactant-stabilised gold nanoparticles, Supramol Sci 4: 329-333.

10. De Roe C, Courtoy PJ, Baudhuin P (1987) A model of protein-colloidal gold interactions. J Histochem Cytochem 35: 1191-1198.

11. Pramanik S, Banerjee P, Sarkar A (2008) Size-dependent interaction of gold nanoparticles with transport protein: A spectroscopic study. J Lumines 128: 1969-1974.

12. Shang L, Wang YZ, Jiang JG (2007) pH-dependent protein conformational changes in albumin: Gold nanoparticle bio-conjugates: A spectroscopic study. Langmuir 23: 2714-2721.

13. Pan B, Cui D, Xu P (2007) Study on interaction between gold nanorod and bovine serum albumin. Colloid Surface A 295: 217-222.

14. Jans H, Liu X, Austin L, Maes G, Huo Q (2009) Dynamic light scattering as a powerful tool for gold nanoparticle bioconjugation and biomolecular binding studies. Anal Chem 81: 9425-9432.

15. Wangoo N, Suri C R, Shekhawat G (2008) Interaction of gold nanoparticles with protein: A spectroscopic study to monitor protein conformational changes. Appl Phys Lett 92: 133104.

16. Naveenraj S, Anandan S, Kathiravan A (2010) The interaction of sonochemically synthesized gold nanoparticles with serum albumins. J Pharm Biomed Anal 53: 804-810.

17. Zhang YZ, Dai J, Xiang X, Li WW, Liu Y (2010) Studies on the interaction between benzidine and bovine serum albumin by spectroscopic methods. Mol Biol Rep 37: 1541-1549.

18. Bi S, Ding L, Tian Y, Song D, Zhou X, et al. (2004) Investigation of the interaction between flavonoids and human serum albumin. J Mol Struct 703: 37-45.

19. Cui Y (2001) Nanowire nanosensors for highly sensitive and selective detection of biological and chemical species. Science 293: 1289-1292.

20. Surewicz WK, Mantsch HH, Chapman D (1993) Determination of protein secondary structure by Fourier transform infrared spectroscopy: A critical assessment. Biochemistry 32: 389-394.

21. Brewer SH, Glomm WR, Johnson MC, Knag MK, Franzen S (2005) Probing BSA binding to citrate-coated gold nanoparticles and surfaces. Langmuir 21: 9303-9307.

22. Gao D, Tian Y, Bi S, Chen Y, Yu A, et al. (2005) Studies on the interaction of colloidal gold and serum albumins by spectral methods. Spectrochim Acta Part A 62: 1203-1208.

23. Ojha B, Das G (2010) The interaction of 5-(alkoxy) naphthalen-1-amine with bovine serum albumin and its effect on the conformation of protein. J Phys Chem B 114: 3979-3986.

24. Bourassa P, Kanakis CD, Tarantilis P, Pollissiou MG, Tajmir-Riahi HA (2010) Resveratrol, genistein, and curcumin bind bovine serum albumin. J Phys Chem B 114: 3348-3354.